ORIGINAL RESEARCH

Environmental impact of multi-wall carbon nanotubes in a novel model of exposure: systemic distribution, macrophage accumulation, and amyloid deposition

Adriana Albini[1,*]
Arianna Pagani[2,3,*]
Laura Pulze[2]
Antonino Bruno[3]
Elisa Principi[3]
Terenzio Congiu[4]
Elisabetta Gini[2,4]
Annalisa Grimaldi[2]
Barbara Bassani[2,3]
Silvio De Flora[5]
Magda de Eguileor[2]
Douglas M Noonan[2,3]

[1]Laboratory of Translational Research, IRCCS Arcispedale Santa Maria Nuova, Reggio Emilia, [2]Department of Biotechnologies and Life Sciences, University of Insubria, Varese, [3]Scientific and Technology Park, IRCCS MultiMedica, Milano, [4]Department of Surgical and Morphological Sciences, University of Insubria, Varese, [5]Department of Health Sciences, University of Genoa, Genoa, Italy

*These authors contributed equally to this work

Correspondence: Douglas M Noonan
Facoltà di Medicina e Chirurgia, Dipartimento di Biotecnologie e Scienze della Vita, Università degli Studi dell'Insubria, Viale Dunant, n 3, 21100 Varese, Italy
Tel +39 332 21 7609
Fax +39 332 21 7609
Mobile +39 34 9147 2227
Email douglas.noonan@uninsubria.it

Abstract: Carbon nanotubes (CNTs) have been extensively investigated and employed for industrial use because of their peculiar physical properties, which make them ideal for many industrial applications. However, rapid growth of CNT employment raises concerns about the potential risks and toxicities for public health, environment, and workers associated with the manufacture and use of these new materials. Here we investigate the main routes of entry following environmental exposure to multi-wall CNTs (MWCNTs; currently the most widely used in industry). We developed a novel murine model that could represent a surrogate of a workplace exposure to MWCNTs. We traced the localization of MWCNTs and their possible role in inducing an innate immune response, inflammation, macrophage recruitment, and inflammatory conditions. Following environmental exposure of CD1 mice, we observed that MWCNTs rapidly enter and disseminate in the organism, initially accumulating in lungs and brain and later reaching the liver and kidney via the bloodstream. Since recent experimental studies show that CNTs are associated with the aggregation process of proteins associated with neurodegenerative diseases, we investigated whether MWCNTs are able to induce amyloid fibril production and accumulation. Amyloid deposits in spatial association with macrophages and MWCNT aggregates were found in the brain, liver, lungs, and kidneys of exposed animals. Our data suggest that accumulation of MWCNTs in different organs is associated with inflammation and amyloid accumulation. In the brain, where we observed rapid accumulation and amyloid fibril deposition, exposure to MWCNTs might enhance progression of neurodegenerative and other amyloid-related diseases. Our data highlight the conclusion that, in a novel rodent model of exposure, MWCNTs may induce macrophage recruitment, activation, and amyloid deposition, causing potential damage to several organs.

Keywords: nanoparticles, animal model, environmental exposure, inflammation, amyloid fibrils, macrophages

Introduction

Nanostructures, a term that includes nanoparticles (NPs), nanotubes, and nanospheres, possess remarkable chemical and physical properties. For these reasons, they are currently manufactured and used in many industrial settings. Carbon nanotubes (CNTs) are one of the most versatile nanomaterials, due to their high tensile strength, ultralight weight, excellent conductibility, and thermal and chemical stabilities. Based on the number of graphene layers, CNTs are classified into single-wall CNTs and multi-wall CNTs (MWCNTs).[1] MWCNTs are widely employed in industry, often as additives in plastics and coatings.

However, reasonable concerns are being expressed about potential risks for workers and other individuals exposed to these novel, non-natural materials, in particular, through their manufacture, use, and disposal.[2–4] In this context, a careful assessment and monitoring is needed for potential unexpected biological interactions and toxicities,[5,6] in particular due to their biopersistence[7–9] and potential for accumulation in organs. CNT toxicity has been reported in rodent models by different routes of administration, such as intratracheal instillation,[8,10–13] inhalation,[14] or intravenous,[15,16] subcutaneous[17] and intraperitoneal injection.[18,19] However, exposure to CNTs is likely to occur simultaneously by multiple routes of entry, as CNTs for their characteristics are able to diffuse in various environmental matrices.[20] For these reasons, we investigated whether and how these NPs are able to enter into the organism and interact with biological systems following external exposure and trigger possible pathological processes resulting from long-term exposure to MWCNTs.

Investigation of toxicities induced by exposure to MWCNTs in vivo has been largely focused on pulmonary effects. The small diameter, the relatively long length, and biopersistence of CNTs have been likened to that of asbestos, and there are extensive concerns regarding the potential pulmonary health hazards of exposure to CNTs.[14,20–23] The effects of pristine (nonfunctionalized) CNTs most commonly involve immune innate reactions, including enhancement of oxidative damage,[24] fibrosis,[13,22,23] collagen-rich granuloma formation,[23] and inflammation.[25–30] When entering biological fluids, CNTs are rapidly coated by proteins, forming a biological protein corona.[31,32] In particular, the hydrophobic interactions between CNTs and proteins could also play a role in inducing proteins to form a cross-sheet, a characteristic of amyloid.[33,34] Amyloid fibrils can self-assemble into large insoluble structures, often associated with toxic properties.[35] Different matrix surfaces can influence amyloidogenesis.[36] In this context, data concerning the ability of CNTs to induce protein aggregation and amyloid fiber formation are controversial.[37–40] The NLRP3 inflammasome, associated with immune responses to CNTs,[27–30,41] activates release of IL-18,[42] a cytokine associated with amyloid plaque formation in Alzheimer's disease,[43–46] a neurodegenerative disorder characterized by amyloid accumulation. For these reasons, we investigated the ability of CNTs to induce amyloid production and deposition in vivo, an innate defense mechanism present in most eukaryotic phyla ranging from fungi and invertebrates[47–49] to humans.[50]

We evaluated the effects of CNTs exposure in a murine model reflecting MWCNTs exposure in the environment.

MWCNTs were added directly within the cage litter twice a week. The animals extensively agitate the litter as part of their normal activities, thus generating an aerosol and thereby exposing the respiratory and digestive tracts as well as skin. This model includes multiple routes of entry, essentially through aerosol inhalation and the digestive tract contact, both direct and indirect (through the physiological process of upper airway CNT trapping and respiratory tract mucus removal). The model can approximate to a workplace exposure to CNTs, where workers can be subjected to an uncontrolled direct and indirect exposure.

We observed that MWCNTs rapidly penetrated into the organism, accumulating as aggregates in the lungs, brain, liver, kidney, and intestine, respectively. We found MWCNTs in the peripheral blood and observed that aggregates of MWCNT were associated with amyloid deposition and macrophage recruitment in most tissues.

Methods
CNT preparation
Commercially available and industrially employed Nanocyl thin MWCNTs NANOCYL™ NC7000 were obtained from Nanocyl (Sambreville, Belgium). The MWCNTs have an average 9.5 nm external diameter by 1.5 µm mean length with a surface area of 250–300 m^2/g. They were manufactured using a catalytic carbon vapor deposition process with a purity of 90%, 10% of metal oxide, and no amorphous carbon. In these experiments, the pristine MWCNTs were used directly without any chemical processing before use.

In vivo study design
The procedures involving animal handling and care conformed to institutional guidelines, in compliance with national and international laws and guidelines for the use of animals in biomedical research, and were approved by the local animal experimentation ethics committee and by the Italian Health Ministry. In this study, 40 male CD1 mice (6–8 weeks of age, Charles River, Calco, Italy) were used. The animals were housed with steel wire tops and corn-cob beddings, maintained in a controlled atmosphere with 12:12 dark–light cycle with free access to food and fresh water. The cages were accommodated in a cabinet equipped with high-efficiency particulate arrestance (HEPA) filters, which acted as a barrier preventing cross-contamination between the exposed and control animals.

In our model, mice were exposed to 1.5 g MWCNTs/80 g litter by adding the dry MWCNTs into the wood shaving cage litter. The MWCNTs were gently mixed with litter, dispersing large aggregates, in order to obtain a homogeneous

dispersion of NPs. Animals (five per cage) were transferred into new cages containing MWCNT/litter twice a week. Controls consisted of animals that were housed similarly but without MWCNTs in the litter. The exposure dose was selected based on previous studies.[51,52] Standard rodent diet, provided as pellets on the top of the cage, and water were provided ad libitum. The animals extensively agitate the litter as part of their normal behavior, thus generating an aerosol that contains MWCNTs and MWCNT-associated dusts, thereby exposing the skin and respiratory and digestive tracts similar to what might be found in an industrial setting using CNTs in an unrestricted and uncontrolled manner. Health status of the animals was monitored by examining skin alterations, reactivity to stimuli, body-weight, as well as food and liquid intake. The mice were sacrificed at 1 week, 2 weeks, 3 weeks, 4 weeks, and 5 weeks after exposure to MWCNTs and organs (lungs, intestine, brain, kidneys, and liver) were excised for subsequent analysis.

Optical and transmission electron microscopy

The liver, lungs, kidneys, intestine, and brains were excised from the animals after the indicated exposure times. Tissue samples for hematoxylin and eosin (H&E), Thioflavin T, or immunofluorescence staining (see below) were embedded in polyfreeze tissue freezing medium (OCT; Polysciences, Inc., Warrington, PA, USA) and immediately frozen in liquid nitrogen. Cryosections (7 μm) were obtained with a Leica CM1850 cryotome. At least 10 samples for each tissue were scored for MWCNT aggregates by counting the aggregates found in five blinded fields for each H&E stained slide using a light microscope. Samples for transmission electron microscopy (TEM) were fixed in 4% glutaraldehyde, washed in 0.1 M cacodylate buffer pH 7.4, and postfixed with 1% osmic acid in cacodylate buffer, pH 7.4. After standard dehydration in ethanol series, samples were embedded in an Epon–Araldite 812 mixture and sectioned with a Reichert Ultracut S ultratome (Leica Microsystems, Wetzlar, Germany). Semithin sections were stained by conventional methods (crystal violet and basic fuchsin) and observed with a light microscope (Nikon Instruments, Melville, NY, USA). Thin sections were stained by uranyl acetate and lead citrate and observed with a JEOL 1010 electron microscope (JEOL, Tokyo, Japan).

Nanotubes detection and localization

To isolate MWCNTs from tissues, the samples from the organs and peripheral blood, obtained after 5 weeks of CNT environmental exposure, were digested in 5 N KOH (Sigma-Aldrich Co., St Louis, MO, USA) for 2 hours to remove all materials of biological origin. The CNTs, being resistant to 5 N KOH, remained after this digestion. The digested material was washed in distilled water to eliminate potassium salts, resuspended in 100 μL of distilled water, and dried onto a cover glass for scanning electron analysis. To enhance CNT signals, the cover glasses were sputter coated with a thin layer of gold and observed in backscattered electron mode with a scanning electron microscope coupled with an energy dispersive X-ray analyzer (EDAX Genesis 2000).

Amyloid fibril characterization

Amyloid structures were identified according to LeVine,[53] by staining with Thioflavin T and detecting the amyloid-specific yellow fluorescence. Cryosections, from selected samples where nanotubes were identified, were rehydrated and stained with 1% Thioflavin T in 0.1 M cloridric acid for 3 minutes at room temperature at dark. Sections were washed with phosphate-buffered saline (PBS), incubated with 1% acetic acid, and after standard dehydration in ethanol series were mounted and observed with an Olympus BH2 microscope through a filter set (excitation wavelength of 465 nm emission). Images were acquired with a DS-5M-L1 Nikon digital camera system. Amyloid structures were confirmed by Congo red staining and birefringence: cryosections were stained for 5 minutes with Congo red solution and hematoxylin, mounted, and observed under a polarized light using an Axioskop 2 microscope (Carl Zeiss Meditec AG, Jena, Germany).

Immunofluorescence

Cryosections (7 μm) from selected samples in which nanotubes were identified were treated for 30 minutes with PBS containing 2% bovine serum albumin (BSA) before the primary antibody incubation (4°C over night). The presence of CD68 (a macrophage marker) was assessed using specific primary antibody (1:100 dilution; Santa Cruz Biotechnology Inc.). After washing, incubation with a suitable secondary antibody conjugated with Cy5 (1:50 dilution; Santa Cruz Biotechnology Inc.) was performed for 90 minutes in a dark humid chamber. The PBS buffer used for washing steps and antibody dilutions contained 2% BSA. In control samples, primary antibody was omitted and samples were treated with BSA-containing PBS. Coverslips were mounted with Citifluor mounting medium and then observed under a fluorescent microscope (Nikon Instruments).

Double-label immunofluorescence

Double-label immunofluorescence was performed to assess which cells were able to produce amyloid fibrils. Cryosections were first stained with Thioflavin T as described above and then incubated with an antibody against CD68. Thioflavin T (in green) and CD68 (in red) signals were observed under a fluorescent microscope (Nikon Instruments).

Statistical analysis

MWCNT aggregates were counted in serial sections stained with H&E of lung, intestine, liver, kidney, and brain of 10 MWCNTs-exposed CD1 mice. Each count is the mean value of five different fields per section observed from multiple animals.

Data were analyzed using GraphPad Prism software (GraphPad Software, Inc., La Jolla, CA, USA) and expressed as mean ± standard error of mean. Statistical analysis was performed using one-way ANOVA. Differences were considered statistically significant when P-values were <0.05.

Results

Exposure of CD1 mice to MWCNTs

Both MWCNT-exposed mice and control mice showed no overt pathological clinical signs. Exposed mice showed a good general health status, with normal reactivity to stimuli and no alterations in body-weight and food and liquid consumption (data not shown). The examination of the directly involved organs (lung and intestinal tract) in MWCNT exposure showed no macroscopic morphological alterations, as compared to controls, except for a darker color in the intestines (data not shown) and darker color of the feces. No macroscopic differences were observed in other organs of exposed mice (data not shown).

Detection of MWCNTs in tissues of exposed mice

Histological examination of sections from lungs, intestinal tract, livers, kidneys, and brains explanted from MWCNT-exposed mice showed patches of dark material, absent in tissue sections from control animals in all tissues examined (Figure 1), that were likely MWCNT aggregates. The dark
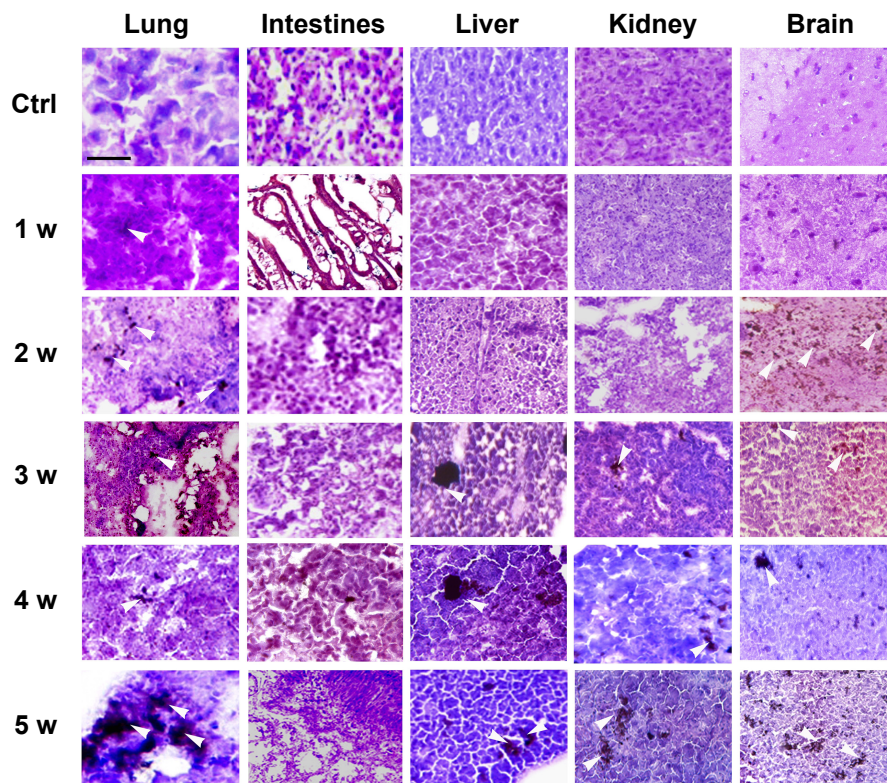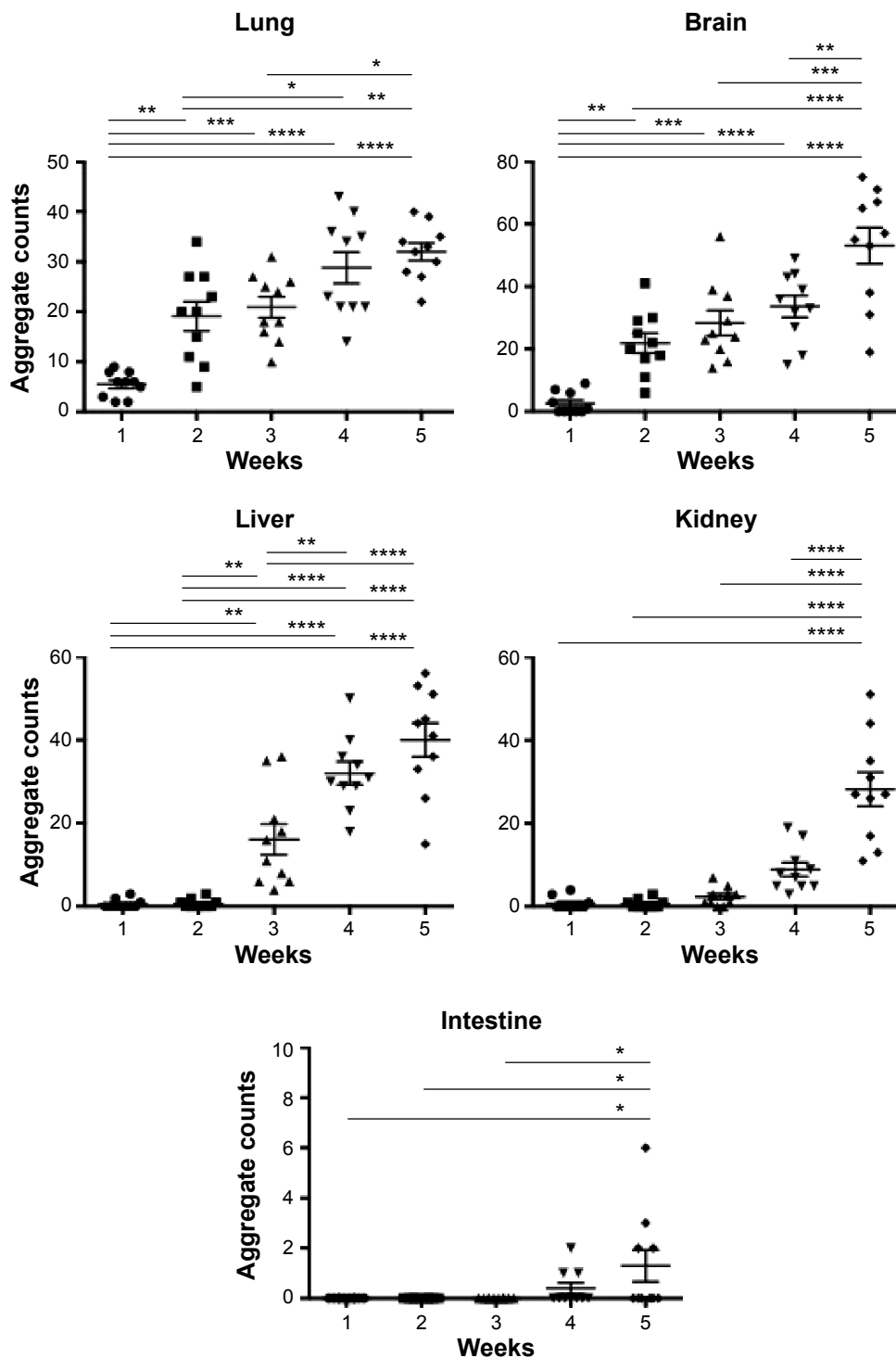

Figure I Histological analysis and quantification of MWCNT aggregates in exposed mice.
Notes: Histological analysis of selected tissues from mice exposed to environmentally administered MWCNTs is shown. Dark deposits (arrowheads) corresponding to MWCNT aggregates were detectable. No dark deposits were observed in tissues from unexposed mice (ctrl); a full panel of representative tissues is shown. The scale bar for all photographs =100 μm.
Abbreviations: MWCNT, multi-wall carbon nanotube; ctrl, control; w, weeks.

aggregates appearing after 1 week of exposure accumulated over time in all tissues; quantification indicated a statistically significant accumulation with substantial differences between tissues (Figure 2). The aggregates were initially found in the lungs since the first week (Figures 1 and 2) indicating that the respiratory tract is a major path of entry. The brains of exposed mice showed similar dark deposits since the second week (Figures 1 and 2) that appeared in

Figure 2 Quantification of the histological analysis of MWCNT aggregates in exposed mice.
Notes: MWCNTs in five random microscopic fields were counted in the lung, liver, brain, kidney, and intestine and provided with relative statistical analysis (*$P<$0.05, **$P<$0.01, ***$P<$0.001, ****$P<$0.0001, as assessed by two-tailed t-tests).
Abbreviation: MWCNT, multi-wall carbon nanotube.

a larger number but less aggregated than those observed in the lungs (Figure 1). Dark aggregates appeared in the liver of mice from the third week of MWCNT exposure (Figures 1 and 2). Aggregates were also detected in the kidneys of mice at late times of exposure (Figures 1 and 2). A similar pattern with accumulation initiating at 4 weeks and becoming statistically significant at 5 weeks, but with a reduced number of MWCNT aggregates, was found in the digestive tract of treated animals (Figures 1 and 2). These data suggest that the digestive tract is not a primary route of entry.

Morphological and chemical conformation of MWCNTs in tissues of exposed mice

The observation of dark deposits in lung, intestine, liver, and brain of MWCNT-exposed mice, not found in unexposed animals, appeared to be directly correlated with the presence of MWCNT aggregates in these organs (Figure 1). TEM and scanning electron microscopy (SEM) analyses, performed on tissues excised from exposed mice, confirmed our hypothesis that the dark deposits observed were effectively MWCNTs. These analyses revealed accumulation of MWCNTs in the lung (Figure 3A–C), liver (Figure 3D–G), and brain (Figure 3H–K). In particular, in the brain of treated animals, MWCNTs were found dispersed both in the vasculature and in association with glial macrophages as demonstrated by TEM analysis (Figure 3H and I), suggesting that macrophages constitute the cells primarily involved in the recognition of this exogenous (nonself) material.

The presence of MWCNTs in mouse tissues was additionally confirmed by taking advantage of the chemical resistance of CNTs. Selected samples from the tissue types where MWCNT aggregates were observed (lung, liver, and brain) from exposed and control groups were minced and digested with 5 N KOH. This treatment removes all materials of biological origin, leaving behind resistant materials, including MWCNTs. The residual KOH-resistant material was collected by centrifugation, washed, and examined by SEM. This material clearly showed the characteristics of CNT aggregates (Figure 3C, G, and K). Similar structures, examined by SEM and TEM, were found in peripheral blood samples (Figure 3L and M) taken from MWCNT-exposed mice. Morphologically, the aggregates derived from chemical digestion of tissue samples were very similar to that obtained from the stock MWCNTs with (Figure 3N) or without (Figure 3O) KOH treatment. No KOH-resistant materials were found in chemically digested tissues or blood from control mice.

SEM and EDAX analysis were performed on previously digested selected samples showing MWCNT aggregates (Figure 3P and Q). EDAX distribution clearly confirmed the presence of carbon (the principal CNT component) that overlaps with MWCNT aggregate present in SEM photos (Figure 3P and Q).

MWCNT aggregates correlate with inflammation

Since CNTs have been reported to be associated with inflammation[3,9–11,14,22,25,28,41,54–56] that in turn is sustained by immune cell recruitment, we evaluated the presence of macrophages (the principal cell type involved) by examining the presence of CD68 positive cells (a common marker for macrophage identification) in association with MWCNT aggregates. The numbers of CD68 positive cells were increased in tissues (lung, brain, liver) in animals exposed to MWCNTs for 5 weeks, particularly in areas where MWCNTs aggregates were localized (Figure 5), suggesting induction of an inflammatory microenvironment.

During oxidative damage and inflammatory process, amyloidogenesis is often induced;[48,49] thus, we investigated whether CNTs aggregation would be associated with the induction of amyloid deposition. The presence of amyloid fibrillar material, revealed by Thioflavin T and Congo red staining, was observed close to MWCNT aggregates. Localization of amyloid fibrils (Figure 4), forming a scaffold around the aggregates of MWCNTs, was found in the 1) lungs (Figure 4A–D) of exposed mice around bronchioles and arteries and 2) liver (Figure 4E–J), near the bile ducts (Figure 4H and J). Amyloid deposition was particularly evident in the 3) brains (Figure 4K–P). We also found evidence of amyloid deposits in the 4) kidney (data not shown) of exposed animals.

The presence of amyloid fibrils was evidenced both by Congo red and Thioflavin T staining. Congo red staining (Figure 4A–D, G, H, M, and N), where the characteristic birefringence under polarized light, was enhanced in MWCNT-exposed animals. Control animals that were not exposed to MWCNTs showed only faint or absent birefringence. Thioflavin T evidenced the presence of amyloidogenic material (in brilliant green) (Figure 4I–J, O, and P).

Double-immunofluorescence staining with Thioflavin T and anti-CD68 antibody (Figure 5) showed a clear co-localization between CD68 positive cells and areas of amyloid deposits in the lung (Figure 5, panel A), brain (Figure 5B), and liver tissues (Figure 5C) of MWCNT-exposed animals, indicating that MWCNT aggregates induce macrophage recruitment, tissue inflammation, and amyloid deposition (Figure 5).
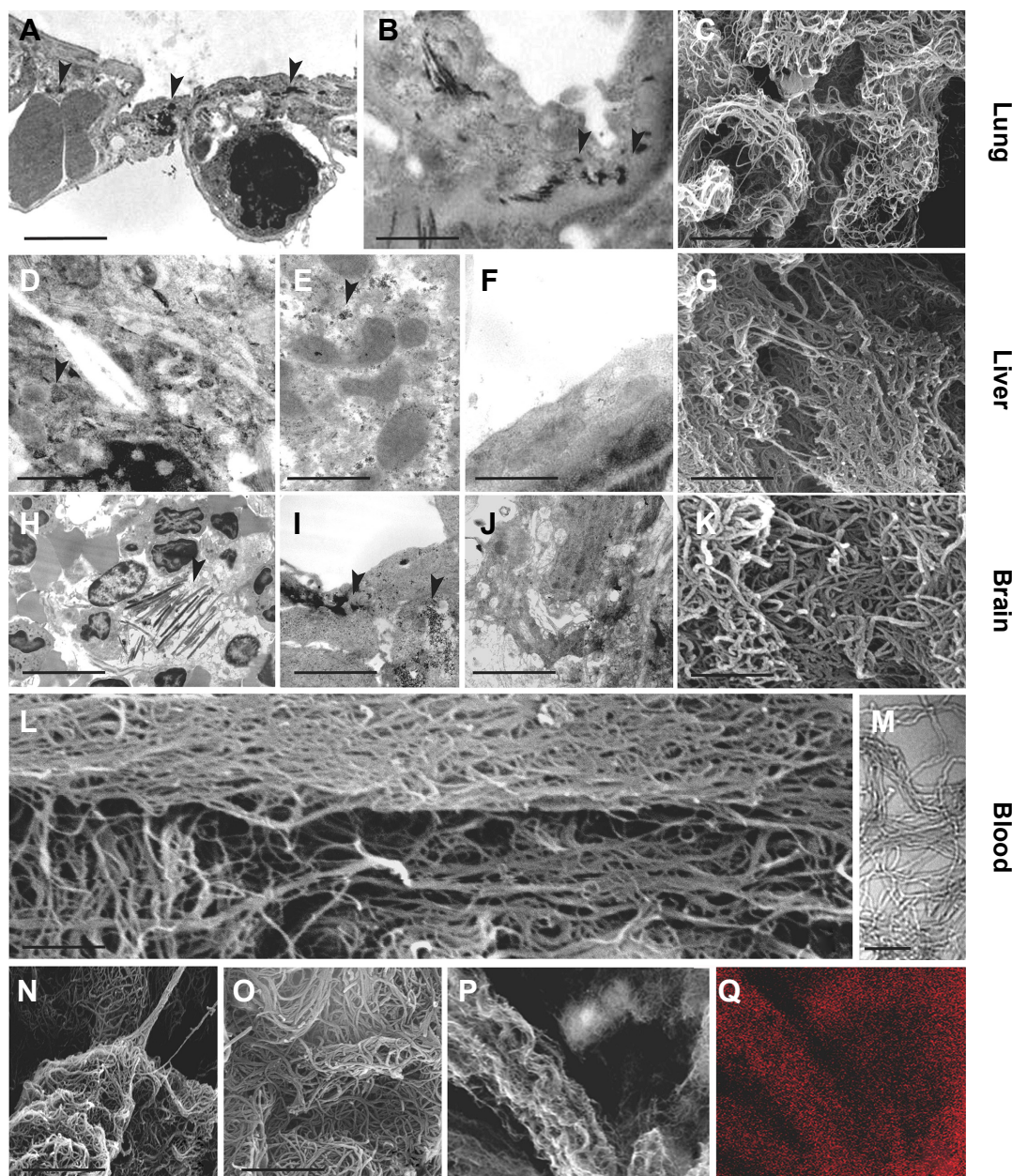
**Figure 3** Ultrastructural analysis of MWCNT aggregates in selected organs.
Notes: TEM and SEM analyses of selected samples of murine tissues showed dark nanoparticle aggregates (arrowheads). Exposed lungs (**A**–**C**), liver (**D**–**G**), and brain (**H**–**K**) in TEM analysis presented dark needle-like structures (arrowheads) with dimensions similar to MWCNTs (**A**, **B**, **D**–**F**). SEM analysis of the KOH-resistant material confirmed the presence of MWCNTs in the lungs (**C**), liver (**G**), brain (**K**), and blood (**L**, **M**) of 5-week MWCNT-exposed animals. These structures were morphologically similar to MWCNT from stock material that has been characterized by SEM before (**N**) and after (**O**) KOH treatment, and were not found in unexposed animals. Combination of SEM analysis of MWCNT obtained by KOH corrosion of exposed liver (**P**) with EDAX (**Q**) clearly showed co-localization of carbon, indicating that the KOH-resistant material was MWCNT aggregates. Scale bars: (**A**) 4.5 μm; (**B**) 1 μm; (**C**) 1 μm; (**D**) 1 μm; (**E**) 1 μm; (**F**) 0.5 μm; (**G**) 1 μm; (**H**) 7.5 μm; (**I**) 2.7 μm; (**J**) 2 μm; (**K**) 0.75 μm; (**L**) 0.5 μm; (**M**) 0.1 μm; (**N**) 1 μm; (**O**) 1 μm.
Abbreviations: TEM, transmission electron microscopy; SEM, scanning electron microscopy; MWCNT, multi-wall carbon nanotubes; EDAX, energy dispersive X-ray analysis.

Discussion

The broad industrial use of CNTs has led to concerns regarding their potential health effects. Models of CNT in vivo pulmonary exposure routes still represent a debated topic. Although inhalation is clearly the most likely route, it is difficult to quantify exposure when using aerosol techniques.[57] Intranasal or intratracheal instillation are the most common administration techniques, but their use focuses on the lungs and may not take into account CNTs trapped in the upper respiratory tract and the subsequent digestive tract exposure. Further, CNTs tend to create large agglomerates when dispersed in aqueous suspension. Taken together, these could lead to an under- or overestimation of the toxicity induced by CNTs. To test the hypothesis that uncontrolled exposure
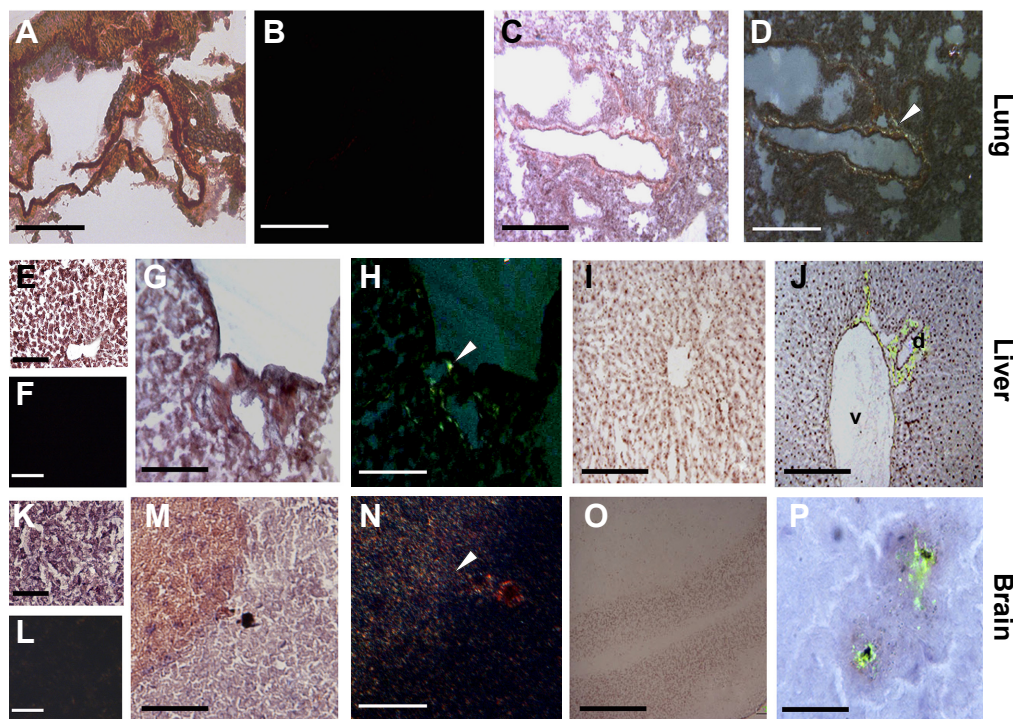
Figure 4 Detection of amyloid fibril deposits by Congo red and Thioflavin T staining.
Notes: In 5-week MWCNT-exposed mice, birefringence (arrowheads) following Congo red staining indicating amyloid deposition was found in the lung (**C**, **D**), liver (**G**, **H**), and brain (**M**, **N**), while these were not found in the same tissues from unexposed mice (**A**, **B**, **E**, **F**, **K**, **L**). In exposed liver (**I**, **J**) Thioflavin T revealed that amyloid fibrils are in association with venules (v) and biliary ducts (d). In the brain (**O**, **P**), the amyloid fibrils surround the MWCNT aggregates in what appears to be a nonself response. The scale bar for all photographs =200 μm.
**Abbreviation:** MWCNT, multi-wall carbon nanotube.

to MWCNTs may adversely affect human health and safety, the route of MWCNTs in exposed animals represents a crucial point to mimic human exposure levels. We propose a novel environmental exposure model that we feel reflects a more realistic scenario of exposure compared to the usual instillation or inhalation procedures explored in several studies. The exposure dose of 18.75 mg/g litter of MWCNT was based on previous exposure studies.[51,52] Further, our model was designed to reflect that of uncontrolled exposure of workers in industrial sectors where MWCNTs are employed, including individual variation due to, among other factors, subjective breathing rate, respiratory mucosal conditions, and direct and indirect contact with NPs and their related dusts. A recent study in a workplace that manufactures MWCNTs indicated exposures to elemental carbon of 5–10 μg/m³.[58] In our model, MWCNT-exposed mice, agitating the litter, generates a NP aerosol that resembles the exposure route of workers who are in contact with NPs in the production process where they are employed, exposing the skin and respiratory and digestive tracts to MWCNTs. Our model reflects in a more realistic manner the subjective differences in MWCNTs exposure. In our model, the lungs were the first organs to show MWCNT accumulation and the digestive tract

the last organ to show accumulation, suggesting that pulmonary exposure represents the predominant route.

We also found MWCNTs in the blood and a rapid distribution to internal organs (brain, liver, kidney), indicating vascular transport. Further, we found a clear time-dependent MWCNT accumulation in all tissues. MWCNT aggregates were found after 1 week of exposure in the brains, indicating a rapid access of CNTs into this tissue. This could be because of either CNTs penetrating the lung and/or digestive tract, entering into the peripheral circulation and then across the blood–brain barrier, or a direct transport from the olfactory nerve into the olfactory bulb[59] and then to the rest of the brain. TEM analysis appeared to confirm this multimodal translocation of MWCNT to the brain as we found MWCNTs associated with brain vessels, dispersed throughout the tissue, and in association with microglia (Figure 2E).

CNTs have been previously associated with foreign body reactions,[21,23] including migration, activation of immune cells and induction of frustrated phagocytosis,[25] and activation of the NLRP3 inflammasome,[3,27–30,41] leading to inflammation.[60] The nanometer scale and needle shape of
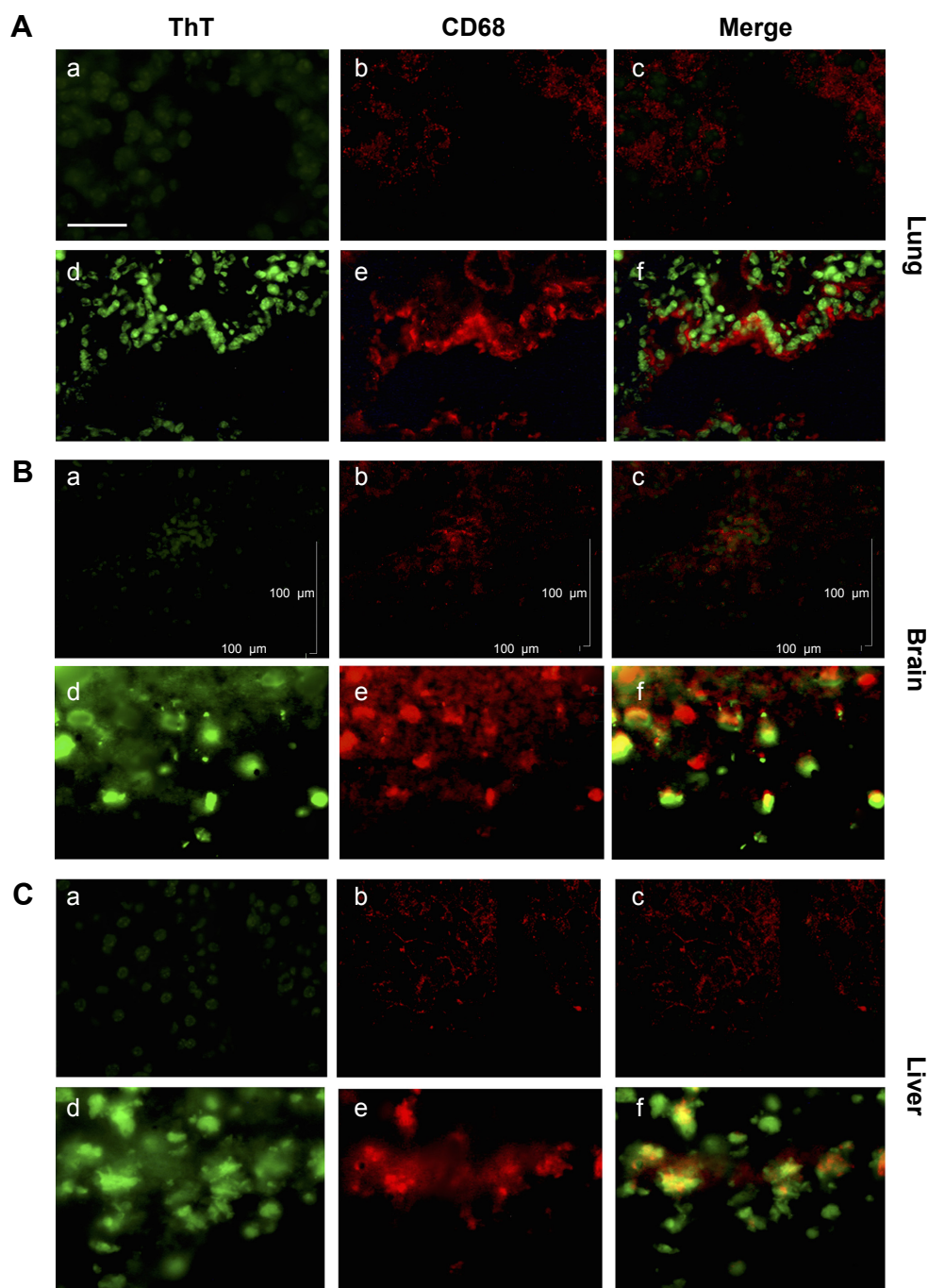
Figure 5 Association between amyloid fibril deposits and macrophage recruitment.
Notes: ThT and anti-CD68 antibody staining revealed co-localization between macrophages and amyloid fibril deposition. In the lung (**A**), brain (**B**), and the liver (**C**) from MWCNT-exposed mice, with respect to the controls (a–c), increased numbers of macrophages are evident in exposed animals (d–f), which are associated with areas of amyloid deposition. The scale bar for all photographs =100 μm.
Abbreviations: ThT, Thioflavin T; MWCNT, multi-wall carbon nanotube.

CNTs recall that of crocidolite asbestos fibers,[54] and CNT administration has been associated with inflammation, fibrosis, and mesothelioma.[19,54,61–66] Interestingly, previous studies documented the formation of granuloma and fibrosis upon pulmonary CNT exposure.[12,14,21,24,25] We did not observe these phenomena in our exposed mice. The results from our CNT-exposed mice are consistent with those reported from observations of workers exposed to MWCNTs, where no overall health aspects were observed even if there was modulation of some biomarkers.[58]

Carboxylated MWCNT cytotoxicity can be reduced if this resistant material is enzymatically degraded.[67,68] Degradation of functionalized CNTs is associated with the degree of carboxylation, and can be obtained using peroxidases, in particular myeloperoxidase and eosinophil peroxidases,[67,68] continued for long periods (80 days). Unlike functionalized CNTs, unmodified pristine CNTs, which we used here, appear to be quite resistant to this type of degradation.[67]

Some of the toxic effects of CNTs have been associated with the presence of metal oxide content used during the manufacturing process.[24] However, one study demonstrated that pulmonary toxicity was found to be independent of metal content.[20] Here we examined industrial-grade pristine MWCNTs since this product is widely used in many industrial processes. In addition, we associate this industrial material to the type of exposure that would be expected of industry workers, mimicking the entry and the possible effects expected. In our model, even with a short exposition schedule (up to 5 weeks), we observed aggregation and deposition of MWCNTs in several organs without macroscopical and/or physiological alterations. Given the association with bile ducts in the liver and the relative hydrophobicity of MWCNTs, a partial clearance through the bile system and physiological elimination in the feces could be considered a possible route of removal. We observed that released and retained feces in MWCNT-exposed mice appeared as much darker material compared to unexposed mice (data not shown). However, this could also be due to oral uptake and digestive tract transit. We note that the intestinal tract was one of the organs where MWCNT aggregates were found much later than many other organs.

Macrophage recruitment and activation due to MWCNT aggregate in different organs is interestingly linked to the production of amyloid fibril formation.[48,49] This primitive defense mechanism employed by cells to aggregate melanin,[37–40,48–50] a strategy employed to build a scaffold for melanin assembly, forming at least a barrier against pathogens or foreign bodies,[48,49] has been recently associated with oxidative damage and inflammation in several different types of cells.[49]

We demonstrate the presence of amyloid in lung, liver, and brain of MWCNT-exposed mice. In our mouse model, amyloid fibril formation in the lungs at the level of the bronchioles and arteries was observed, suggesting the presence and the passage of MWCNTs into the bloodstream, as also shown by treating whole blood with KOH. In vitro CNTs have been shown to transiently interact with endothelial cells and pass through the acidic lysosomal compartment,[69] consistently with the macrophage response to different types of CNTs.[70] In the brain, amyloid was localized around aggregates of MWCNT, indicating that amyloid deposition might be a barrier to contain nonself material. Further, in the livers of exposed animals, we observed amyloid fibrils associated with biliary ducts but absent in the parenchyma. A spatial association between macrophages, amyloid deposition, and MWCNT aggregates was found in exposed lung, liver, and brain,[71] suggesting that MWCNTs could potentially be involved in promoting neurodegenerative and other amyloid-associated diseases.

Conclusion

Our data reveal that CNTs can rapidly enter and disseminate in the organism after environmental exposure in a novel model system. The observed pharmacokinetic patterns suggest that, according to a first-pass effect mechanism, inhalation represents the main exposure route under our experimental conditions. The data indicate that the major organs affected are not only the lungs but also the brain and liver, where the accumulation results in inflammation and amyloid deposition. Clinically, secondary amyloidosis is associated with chronic inflammatory conditions and is characterized by a clinically silent phase followed by overt clinical signs depending on the organ(s) involved. A long-term cytotoxicity due to CNT presence in the liver and in the central nervous system could promote several pathologies, such as cirrhosis or neurodegenerative diseases associated with amyloid deposits (in particular, in subjects with other risk factors). These data highlight new aspects of the potential risks for public health linked to environmental diffusion of CNTs and human exposure.

Acknowledgments

Author contributions

AA, DMN, AG, and MDE conceived the experiments, performed the statistical analysis, and wrote the manuscript. AP, LP, EP, and EG performed the in vivo and in vitro experiments. TC performed the SEM analysis. AB and BB contributed to the in vivo experiments, performed the statistical analysis, and wrote the manuscript. SDF analyzed the data and critically revised the manuscript. All authors contributed toward data analysis, drafting, and critically revising the paper and agree to be accountable for all aspects of the work.

Disclosure

The authors report no conflicts of interest in this work.

References

1. Liu Z, Tabakman S, Welsher K, Dai H. Carbon nanotubes in biology and medicine: in vitro and in vivo detection, imaging and drug delivery. *Nano Res*. 2009;2(2):85–120.
2. Hristozov DR, Gottardo S, Cinelli M, et al. Application of a quantitative weight of evidence approach for ranking and prioritising occupational exposure scenarios for titanium dioxide and carbon nanomaterials. *Nanotoxicology*. 2014;8(2):117–131.
3. Johnston H, Pojana G, Zuin S, et al. Engineered nanomaterial risk. Lessons learnt from completed nanotoxicology studies: potential solutions to current and future challenges. *Crit Rev Toxicol*. 2013;43(1):1–20.
4. Winkler DA, Mombelli E, Pietroiusti A, et al. Applying quantitative structure-activity relationship approaches to nanotoxicology: current status and future potential. *Toxicology*. 2013;313(1):15–23.
5. Guadagnini R, Halamoda Kenzaoui B, Walker L, et al. Toxicity screenings of nanomaterials: challenges due to interference with assay processes and components of classic in vitro tests. *Nanotoxicology*. 2015;9:13–24.
6. Donaldson K, Stone V, Tran CL, Kreyling W, Borm PJ. Nanotoxicology. *Occup Environ Med*. 2004;61(9):727–728.
7. Donaldson K, Murphy F, Schinwald A, Duffin R, Poland CA. Identifying the pulmonary hazard of high aspect ratio nanoparticles to enable their safety-by-design. *Nanomedicine (Lond)*. 2011;6(1):143–156.
8. Elgrabli D, Floriani M, Abella-Gallart S, et al. Biodistribution and clearance of instilled carbon nanotubes in rat lung. *Part Fibre Toxicol*. 2008; 5:20.
9. Osmond-McLeod MJ, Poland CA, Murphy F, et al. Durability and inflammogenic impact of carbon nanotubes compared with asbestos fibres. *Part Fibre Toxicol*. 2011;8:15.
10. Inoue K, Koike E, Yanagisawa R, Hirano S, Nishikawa M, Takano H. Effects of multi-walled carbon nanotubes on a murine allergic airway inflammation model. *Toxicol Appl Pharmacol*. 2009;237(3):306–316.
11. Inoue K, Yanagisawa R, Koike E, Nishikawa M, Takano H. Repeated pulmonary exposure to single-walled carbon nanotubes exacerbates allergic inflammation of the airway: possible role of oxidative stress. *Free Radic Biol Med*. 2010;48(7):924–934.
12. Lam CW, James JT, McCluskey R, Hunter RL. Pulmonary toxicity of single-wall carbon nanotubes in mice 7 and 90 days after intratracheal instillation. *Toxicol Sci*. 2004;77(1):126–134.
13. Poulsen SS, Saber AT, Williams A, et al. MWCNTs of different physicochemical properties cause similar inflammatory responses, but differences in transcriptional and histological markers of fibrosis in mouse lungs. *Toxicol Appl Pharmacol*. 2014;284(1):16–32.
14. Shvedova AA, Kisin E, Murray AR, et al. Inhalation vs aspiration of single-walled carbon nanotubes in C57BL/6 mice: inflammation, fibrosis, oxidative stress, and mutagenesis. *Am J Physiol Lung Cell Mol Physiol*. 2008;295(4):L552–L565.
15. Ji Z, Zhang D, Li L, et al. The hepatotoxicity of multi-walled carbon nanotubes in mice. *Nanotechnology*. 2009;20(44):445101.
16. Yang ST, Wang X, Jia G, et al. Long-term accumulation and low toxicity of single-walled carbon nanotubes in intravenously exposed mice. *Toxicol Lett*. 2008;181(3):182–189.
17. Patlolla A, McGinnis B, Tchounwou P. Biochemical and histopathological evaluation of functionalized single-walled carbon nanotubes in Swiss-Webster mice. *J Appl Toxicol*. 2011;31(1):75–83.
18. Patlolla AK, Berry A, Tchounwou PB. Study of hepatotoxicity and oxidative stress in male Swiss-Webster mice exposed to functionalized multi-walled carbon nanotubes. *Mol Cell Biochem*. 2011; 358(1–2):189–199.
19. Rittinghausen S, Hackbarth A, Creutzenberg O, et al. The carcinogenic effect of various multi-walled carbon nanotubes (MWCNTs) after intraperitoneal injection in rats. *Part Fibre Toxicol*. 2014;11(1):59.
20. Lam CW, James JT, McCluskey R, Arepalli S, Hunter RL. A review of carbon nanotube toxicity and assessment of potential occupational and environmental health risks. *Crit Rev Toxicol*. 2006;36(3):189–217.
21. Warheit DB, Laurence BR, Reed KL, Roach DH, Reynolds GA, Webb TR. Comparative pulmonary toxicity assessment of single-wall carbon nanotubes in rats. *Toxicol Sci*. 2004;77(1):117–125.
22. Shvedova AA, Kisin ER, Mercer R, et al. Unusual inflammatory and fibrogenic pulmonary responses to single-walled carbon nanotubes in mice. *Am J Physiol Lung Cell Mol Physiol*. 2005;289(5):L698–L708.
23. Muller J, Huaux F, Moreau N, et al. Respiratory toxicity of multi-wall carbon nanotubes. *Toxicol Appl Pharmacol*. 2005;207(3):221–231.
24. Pulskamp K, Diabate S, Krug HF. Carbon nanotubes show no sign of acute toxicity but induce intracellular reactive oxygen species in dependence on contaminants. *Toxicol Lett*. 2007;168(1):58–74.
25. Brown D, Kinloch I, Bangert U, et al. An in vitro study of the potential of carbon nanotubes and nanofibres to induce inflammatory mediators and frustrated phagocytosis. *Carbon N Y*. 2007;45:1743–1756.
26. Donaldson K, Schinwald A, Murphy F, et al. The biologically effective dose in inhalation nanotoxicology. *Acc Chem Res*. 2013;46(3): 723–732.
27. Hussain S, Sangtian S, Anderson SM, et al. Inflammasome activation in airway epithelial cells after multi-walled carbon nanotube exposure mediates a profibrotic response in lung fibroblasts. *Part Fibre Toxicol*. 2014;11:28.
28. Jessop F, Holian A. Extracellular HMGB1 regulates multi-walled carbon nanotube-induced inflammation in vivo. *Nanotoxicology*. 2014; 9:1–8.
29. Girtsman TA, Beamer CA, Wu N, Buford M, Holian A. IL-1R signalling is critical for regulation of multi-walled carbon nanotubes-induced acute lung inflammation in C57Bl/6 mice. *Nanotoxicology*. 2014;8(1): 17–27.
30. Meunier E, Coste A, Olagnier D, et al. Double-walled carbon nanotubes trigger IL-1beta release in human monocytes through Nlrp3 inflammasome activation. *Nanomedicine*. 2012;8(6):987–995.
31. Ge C, Du J, Zhao L, et al. Binding of blood proteins to carbon nanotubes reduces cytotoxicity. *Proc Natl Acad Sci U S A*. 2011;108(41): 16968–16973.
32. Walkey CD, Chan WC. Understanding and controlling the interaction of nanomaterials with proteins in a physiological environment. *Chem Soc Rev*. 2012;41(7):2780–2799.
33. Chiti F, Dobson CM. Protein misfolding, functional amyloid, and human disease. *Annu Rev Biochem*. 2006;75:333–366.
34. Koo EH, Lansbury PT Jr, Kelly JW. Amyloid diseases: abnormal protein aggregation in neurodegeneration. *Proc Natl Acad Sci U S A*. 1999; 96(18):9989–9990.
35. Baglioni S, Casamenti F, Bucciantini M, et al. Prefibrillar amyloid aggregates could be generic toxins in higher organisms. *J Neurosci*. 2006; 26(31):8160–8167.
36. Kowalewski T, Holtzman DM. In situ atomic force microscopy study of Alzheimer's beta-amyloid peptide on different substrates: new insights into mechanism of beta-sheet formation. *Proc Natl Acad Sci U S A*. 1999; 96(7):3688–3693.

37. Guo J, Li J, Zhang Y, Jin X, Liu H, Yao X. Exploring the influence of carbon nanoparticles on the formation of beta-sheet-rich oligomers of IAPP(2)(2)(-)(2)(8) peptide by molecular dynamics simulation. *PLoS One*. 2013;8(6):e65579.

38. Li H, Luo Y, Derreumaux P, Wei G. Carbon nanotube inhibits the formation of beta-sheet-rich oligomers of the Alzheimer's amyloid-beta(16–22) peptide. *Biophys J*. 2011;101(9):2267–2276.

39. Linse S, Cabaleiro-Lago C, Xue WF, et al. Nucleation of protein fibrillation by nanoparticles. *Proc Natl Acad Sci U S A*. 2007; 104(21): 8691–8696.

40. Luo J, Warmlander SK, Yu CH, Muhammad K, Graslund A, Pieter Abrahams J. The Abeta peptide forms non-amyloid fibrils in the presence of carbon nanotubes. *Nanoscale*. 2014;6(12):6720–6726.

41. Palomäki J, Välimäki E, Sund J, et al. Long, needle-like carbon nanotubes and asbestos activate the NLRP3 inflammasome through a similar mechanism. *ACS Nano*. 2011;5(9):6861–6870.

42. Lawlor KE, Vince JE. Ambiguities in NLRP3 inflammasome regulation: is there a role for mitochondria? *Biochim Biophys Acta*. 2014;1840(4): 1433–1440.

43. Bossù P, Ciaramella A, Salani F, et al. Interleukin-18, from neuroinflammation to Alzheimer's disease. *Curr Pharm Des*. 2010;16(38): 4213–4224.

44. Ojala J, Alafuzoff I, Herukka SK, van Groen T, Tanila H, Pirttila T. Expression of interleukin-18 is increased in the brains of Alzheimer's disease patients. *Neurobiol Aging*. 2009;30(2):198–209.

45. Sutinen EM, Pirttila T, Anderson G, Salminen A, Ojala JO. Proinflammatory interleukin-18 increases Alzheimer's disease-associated amyloid-beta production in human neuron-like cells. *J Neuroinflammation*. 2012;9:199.

46. Swardfager W, Lanctot K, Rothenburg L, Wong A, Cappell J, Herrmann N. A meta-analysis of cytokines in Alzheimer's disease. *Biol Psychiatry*. 2010;68(10):930–941.

47. Falabella P, Riviello L, Pascale M, et al. Functional amyloids in insect immune response. *Insect Biochem Mol Biol*. 2012;42(3):203–211.

48. Grimaldi A, Tettamanti G, Congiu T, et al. The main actors involved in parasitization of Heliothis virescens larva. *Cell Tissue Res*. 2012;350(3): 491–502.

49. Grimaldi A, Girardello R, Malagoli D, et al. Amyloid/Melanin distinctive mark in invertebrate immunity. *Invertebrate Surviv J*. 2012;9: 153–162.

50. Fowler DM, Koulov AV, Alory-Jost C, Marks MS, Balch WE, Kelly JW. Functional amyloid formation within mammalian tissue. *PLoS Biol*. 2006;4(1):e6.

51. Porter DW, Hubbs AF, Mercer RR, et al. Mouse pulmonary dose- and time course-responses induced by exposure to multi-walled carbon nanotubes. *Toxicology*. 2010;269(2–3):136–147.

52. NIOSH. In: Services DoHAH, editor. *Occupation Exposure to Carbon Nanotubes and Nanofibers*. Vol. 65. Atlanta: Centers for Disease Control and Prevention and National Institute for Occupational Safety and Health; 2013. Available from: http://www.cdc.gov/niosh/docs/2013-145/pdfs/2013-145.pdf

53. LeVine H 3rd. Quantification of beta-sheet amyloid fibril structures with thioflavin T. *Methods Enzymol*. 1999;309:274–284.

54. Donaldson K, Murphy FA, Duffin R, Poland CA. Asbestos, carbon nanotubes and the pleural mesothelium: a review of the hypothesis regarding the role of long fibre retention in the parietal pleura, inflammation and mesothelioma. *Part Fibre Toxicol*. 2010;7:5.

55. Dostert C, Petrilli V, Van Bruggen R, Steele C, Mossman BT, Tschopp J. Innate immune activation through Nalp3 inflammasome sensing of asbestos and silica. *Science*. 2008;320(5876):674–677.

56. Grecco AC, Paula RF, Mizutani E, et al. Up-regulation of T lymphocyte and antibody production by inflammatory cytokines released by macrophage exposure to multi-walled carbon nanotubes. *Nanotechnology*. 2011;22(26):265103.

57. Maynard A, Aitken R. Assessing exposure to airborne nanomaterials: current abilities and future requirements. *Nanotoxicology*. 2007;1: 26–41.

58. Lee JS, Choi YC, Shin JH, et al. Health surveillance study of workers who manufacture multi-walled carbon nanotubes. *Nanotoxicology*. 2014; 9:1–10.

59. Oberdörster G, Sharp Z, Atudorei V, et al. Translocation of inhaled ultrafine particles to the brain. *Inhal Toxicol*. 2004;16(6–7):437–445.

60. Dong J, Ma Q. Advances in mechanisms and signaling pathways of carbon nanotube toxicity. *Nanotoxicology*. 2015;9:1–19.

61. Poland CA, Duffin R, Kinloch I, et al. Carbon nanotubes introduced into the abdominal cavity of mice show asbestos-like pathogenicity in a pilot study. *Nat Nanotechnol*. 2008;3(7):423–428.

62. Sakamoto Y, Nakae D, Fukumori N, et al. Induction of mesothelioma by a single intrascrotal administration of multi-wall carbon nanotube in intact male Fischer 344 rats. *J Toxicol Sci*. 2009;34(1):65–76.

63. Sun B, Wang X, Ji Z, et al. NADPH oxidase-dependent NLRP3 inflammasome activation and its important role in lung fibrosis by multiwalled carbon nanotubes. *Small*. 2015;11(17):2087–2097.

64. Takagi A, Hirose A, Futakuchi M, Tsuda H, Kanno J. Dose-dependent mesothelioma induction by intraperitoneal administration of multi-wall carbon nanotubes in p53 heterozygous mice. *Cancer Sci*. 2012; 103(8):1440–1444.

65. Takagi A, Hirose A, Nishimura T, et al. Induction of mesothelioma in p53+/− mouse by intraperitoneal application of multi-wall carbon nanotube. *J Toxicol Sci*. 2008;33(1):105–116.

66. Varga C, Szendi K. Carbon nanotubes induce granulomas but not mesotheliomas. *In Vivo*. 2010;24(2):153–156.

67. Kotchey GP, Zhao Y, Kagan VE, Star A. Peroxidase-mediated biodegradation of carbon nanotubes in vitro and in vivo. *Adv Drug Deliv Rev*. 2013;65(15):1921–1932.

68. Zhao Y, Allen BL, Star A. Enzymatic degradation of multiwalled carbon nanotubes. *J Phys Chem A*. 2011;115(34):9536–9544.

69. Albini A, Mussi V, Parodi A, et al. Interactions of single-wall carbon nanotubes with endothelial cells. *Nanomedicine*. 2010;6(2):277–288.

70. Palomäki J, Sund J, Vippola M, et al. A secretomics analysis reveals major differences in the macrophage responses towards different types of carbon nanotubes. *Nanotoxicology*. 2014;8:1–10.

71. Lai AY, McLaurin J. Clearance of amyloid-beta peptides by microglia and macrophages: the issue of what, when and where. *Future Neurol*. 2012; 7(2):165–176.

→ Video abstract

Point your SmartPhone at the code above. If you have a
QR code reader the video abstract will appear. Or use:

http://youtu.be/foozY7o_QEk

International Journal of Nanomedicine

Publish your work in this journal

The International Journal of Nanomedicine is an international, peer-reviewed journal focusing on the application of nanotechnology in diagnostics, therapeutics, and drug delivery systems throughout the biomedical field. This journal is indexed on PubMed Central, MedLine, CAS, SciSearch®, Current Contents®/Clinical Medicine, Journal Citation Reports/Science Edition, EMBase, Scopus and the Elsevier Bibliographic databases. The manuscript management system is completely online and includes a very quick and fair peer-review system, which is all easy to use. Visit http://www.dovepress.com/testimonials.php to read real quotes from published authors.

Submit your manuscript here: http://www.dovepress.com/international-journal-of-nanomedicine-journal

Dovepress